Long-Term-Infected Telomerase-Immortalized Endothelial Cells: a Model for Kaposi's Sarcoma-Associated Herpesvirus Latency In Vitro and In Vivo†

Feng-Qi An,[2] Hope Merlene Folarin,[2] Nicole Compitello,[2] Justin Roth,[2] Stanton L. Gerson,[2]
Keith R. McCrae,[2] Farnaz D. Fakhari,[3] Dirk P. Dittmer,[3] and Rolf Renne[1]*

*Department of Molecular Genetics and Microbiology and University of Florida Shands Cancer Center, University of Florida,
Gainesville, Florida 32610[1]; Division of Hematology/Oncology, Case Western Reserve University, Cleveland,
Ohio 44106[2]; and Lineberger Comprehensive Cancer Center and Department of Microbiology and
Immunology, University of North Carolina at Chapel Hill, Chapel Hill, North Carolina 27599[3]*

Kaposi's sarcoma-associated herpesvirus (KSHV) is associated with Kaposi's sarcoma (KS), primary effusion lymphoma (PEL), and multicentric Castleman's disease. Most KS tumor cells are latently infected with KSHV and are of endothelial origin. While PEL-derived cell lines maintain KSHV indefinitely, all KS tumor-derived cells to date have lost viral genomes upon ex vivo cultivation. To study KSHV latency and tumorigenesis in endothelial cells, we generated *t*elomerase-*i*mmortalized human umbilical *v*ein *e*ndothelial (TIVE) cells. TIVE cells express all KSHV latent genes 48 h postinfection, and productive lytic replication could be induced by RTA/Orf50. Similar to prior models, infected cultures gradually lost viral episomes. However, we also obtained, for the first time, two endothelial cell lines in which KSHV episomes were maintained indefinitely in the absence of selection. Long-term KSHV maintenance correlated with loss of reactivation in response to RTA/Orf50 and complete oncogenic transformation. Long-term-infected TIVE cells (LTC) grew in soft agar and proliferated under reduced-serum conditions. LTC, but not parental TIVE cells, formed tumors in nude mice. These tumors expressed high levels of the latency-associated nuclear antigen (LANA) and expressed lymphatic endothelial specific antigens as found in KS (LYVE-1). Furthermore, host genes, like those encoding interleukin 6, vascular endothelial growth factor, and basic fibroblast growth factor, known to be highly expressed in KS lesions were also induced in LTC-derived tumors. KSHV-infected LTCs represent the first xenograft model for KS and should be of use to study KS pathogenesis and for the validation of anti-KS drug candidates.

Kaposi's sarcoma-associated herpesvirus (KSHV), also called human herpesvirus 8 (HHV-8), is believed to be the causative agent for Kaposi's sarcoma (KS) (for a review, see references 1 and 27). Within KS tumor lesions, the majority of cells express endothelial markers and are latently infected with KSHV, as defined by the presence of the circular viral genome and limited viral-gene expression. Studying KSHV's role in KS is complicated by the fact that cells explanted from KS lesions lose the KSHV genome after several cell divisions in culture (2, 43). In addition to KS, KSHV is associated with two lymphoproliferative diseases: primary effusion lymphomas (PEL) and multicentric Castleman's disease (MCD) (11, 59). In contrast to KS lesions, PEL-derived cell lines that are latently infected with KSHV are readily established in culture. These cells maintain viral episomes indefinitely and remain dependent on KSHV for survival (31, 33). Therefore, many aspects of KSHV biology have been studied in PEL-derived cell lines rather than in endothelial cells (56; for a review, see reference 1).

Several endothelial-cell-derived tissue culture models have been described. Common to these models, which are based on

dermal microvascular endothelial cells (DMVEC), are their susceptibility to cell-free infection with PEL-derived KSHV and their capability to support lytic replication, both spontaneously and upon induction with the phorbol ester tetradecanoyl phorbol acetate (TPA) (13, 23, 41, 48). With respect to the maintenance of latency and the induction of phenotypic changes following KSHV infection, significant differences have been reported: (i) telomerase-immortalized microvascular endothelial (TIME) cells are susceptible to KSHV infection but cannot support long-term episomal maintenance (41), and (ii) Ciufo et al. reported on persistent infections in primary DMVEC consisting of a mixture of latently and lytically infected cells. Because both the formation of spindle cells and the number of latently infected latency-associated nuclear antigen (LANA)-expressing cells decreased in the presence of phosphoformic acid (PFA), an inhibitor of lytic DNA replication, these data suggested that lytic replication and reinfection contributed to long-term viral persistence (13, 38). Supporting this model, Grundhoff and Ganem demonstrated that most epithelial and endothelial cell types fail to efficiently support stable latency after in vitro infection (32). DMVEC immortalized by the papillomavirus proteins E6/E7 (targeting the major tumor suppressor proteins p53 and pRB) and infected by KSHV exhibit spindle cell formation and outgrowth of cells with altered attachment requirements and changes in host cell gene expression, such as up-regulation of c-Kit. Such changes

were observed by maintaining these cells under long-term culture (48). Finally, primary bone marrow-derived endothelial cells were transformed after KSHV infection in vitro. This model was the first to highlight the paracrine effects of KSHV infection. In this system, too, KSHV is gradually lost, and less than 5% of cells in a mixed culture remain KSHV infected (23).

Here, we report on a novel umbilical-cord-derived vein endothelial-cell model that is highly susceptible to KSHV and supported high-level lytic replication early after infection. Most cells lost the viral episomes over time; however, we also obtained telomerase-immortalized human umbilical-vein endothelial (TIVE) cell cultures that stably support KSHV latency in the absence of selection and that underwent marked phenotypical changes. Long-term-infected TIVE cells (LTC), but not uninfected TIVE cells, formed colonies in soft agar and efficiently induced tumor formation in nude mice. Analysis of these tumors revealed histological features and expression of the same surface markers that define KS tumors. Hence, LTC provide a novel and unique model to study KSHV pathogenesis in vivo in a human endothelial-cell-specific manner.

MATERIALS AND METHODS

Primary cells, cell lines, and KSHV stocks. Umbilical cord-derived endothelial cells were isolated by collagenase treatment and grown in Fisher M199 medium supplemented with 15% fetal calf serum (FCS) and 5 ml of filtered endothelial-cell growth factors (ECGF) as previously described (30). The primary effusion lymphoma line BCBL-1, as well as the procedures for inducing and harvesting KSHV virions, have been described previously (54). Infections of TIVE cells were done in the presence of Polybrene (4 µg/ml), as previously described (41).

Vectors and retroviral transduction. pBabe/puro/hTert was kindly provided by Robert Weinberg (Massachusetts Institute of Technology). As a control, we used MFG-GFP vector. Ten micrograms of each vector was cotransfected with 15 µg of pVSV-G for pseudotyping into Phoenix-Ampho packaging cells (kindly provided by Garry Nolan, Stanford University). The supernatants were harvested 48 h posttransfection and filtered, and NIH 3T3 cells were used to determine viral titers. For transduction of human vein endothelial cells (HUVEC), cells at 50% confluence were incubated with human telomerase reverse transcriptase (hTert) or green fluorescent protein (GFP) virus in the presence of Polybrene (8 µg/ml) for 8 h. Virus-containing medium was replaced with new virus and incubated for a second period of 12 h, after which the medium was replaced with fresh medium. Three days postinfection, the cells were divided into two flasks, and one was puromycin treated. To monitor life spans, MFG-GFP-transduced HUVEC and nontransduced cells from the same primary cell preparation were cultivated in parallel.

Analysis of viral gene products and cellular surface markers. Immunofluorescence assays and Western blot analysis for LANA and K8.1 were performed as previously described (12). Antibodies were kindly provided by Don Ganem (University of California—San Francisco) and Bala Chandran (University of Kansas).

Immunohistochemical analyses were performed using commercially available antibodies against CD31, CD34, CD45, CD68, CD105, Flt, keratin, SMSA, UEA, S100A10, and factor VIII (also called von Willebrand factor [vWF]). For development, a secondary antibody conjugated to alkaline phosphatase was used. Tumors were removed and fixed in 10% neutral buffered formalin (Fisher Diagnostic) for 2 days, embedded in paraffin blocks, and processed by routine methods, and 5-µm sections were obtained. Dewaxed sections were microwaved in 1 mM EDTA (pH 8) for PCNA and lymphatic endothelial specific antigens as found in KS (LYVE-1) and Retrievagen A (BD Pharmingen, San Diego, CA) for rabbit polyclonal antibody to LANA of HHV-8 for 15 min, cooled, and treated with 3% H_2O_2 (Sigma) in 10% methanol to inhibit endogenous peroxidase activity, blocked with blocking solution with 10% horse serum (Vector Laboratories, Burlingame, CA), and incubated overnight with the appropriate primary antibody at 1:200 dilution. PCNA (FL-261) rabbit polyclonal immunoglobulin G was purchased from Santa Cruz Biotechnology (Santa Cruz, CA); anti-LYVE-1 rabbit immunoaffinity-purified immunoglobulin G was purchased from Upstate (Lake Placid, NY); rabbit polyclonal antibody to LANA of HHV-8 was from D. Ganem; and phosphate-buffered saline (PBS) was used as the negative control. After being washed, sections were stained for 1 h with a goat anti-rabbit biotinylated horseradish peroxidase H-conjugated secondary antibody, followed by Avidin DH (VECTASTAIN ABC kit; Vector Laboratories, Burlingame, CA). The sections were washed in PBS and incubated for 5 min with Vector NovaRed substrate for peroxidase (Vector Laboratories, Burlingame, CA). The slides were counterstained with hematoxylin (Sigma).

Colony formation in soft agar. First, a base layer containing 0.5% agarose medium and 5% FCS was poured into six-well plates. Then, 10,000 cells were mixed with 0.4% agarose in Earl's minimal essential medium (EMEM) containing 5% FCS to form a single-cell suspension. After being seeded, the plates were incubated for 2 weeks. To establish clones, single colonies were picked and transferred into 96-well plates for expansion.

Mouse tumorigenesis assays. Cells were counted and washed once in ice-cold PBS (Cellgro Mediatech, Inc., Herndon, VA), and the indicated cell doses were diluted in 50 µl PBS plus 50 µl growth factor-depleted Matrigel (BD Biosciences, Bedford, MA). Cells were injected subcutaneously into the right flanks of nude BALB/c mice (Taconic, Inc., Germantown, NJ). The mice were observed every day for the presence of palpable tumors. The tumors were excised from the site of injection and were either fixed in formalin (Fisher Diagnostics, Middletown, VA) or resuspended in TRI reagent (Sigma-Aldrich Corp., St. Louis, MO) and processed for reverse transcription (RT)-PCR.

Flow cytometry analysis. To determine the DNA content, cells were fixed and DNA was stained with propidium iodide prior to flow cytometry analysis using a FACScan analyzer (Becton Dickinson, Mountain View, CA). Data were analyzed using ModFit Lt V3 software (Verity Software House).

Gardella gel analysis. To prove episomal genome maintenance, 50,000 to 100,000 long-term-infected TIVE cells and BCBL-1 cells (TPA treated) as controls were loaded into lysis buffer, electrophoresed on vertical 0.8% agarose gels, transferred to membranes, and analyzed by Southern blotting as previously described (55).

KSHV array analysis. Poly(A) mRNA of TIVE cells, KSHV-infected TIVE cells at 3 months and 10 months, KSHV-infected long-term culture SLK cells, and BCBL-1 cells were prepared and subjected to real-time RT-PCR using the previously published KSHV array and procedures (50). Solid tumor pieces were resuspended in 750 µl TRI Reagent (Sigma-Aldrich Corp., St. Louis, MO) and disrupted using an Ultra-Turrax T8 (IKA Labortechnik, Germany). RNA was isolated according to the supplier's protocol, precipitated, and resuspended in 50 µl diethyl pyrocarbonate-treated water at 56°C for 10 min. The RNA was reverse transcribed as described previously (3) in a 20-µl reaction mixture with 100 U of Moloney murine leukemia virus reverse transcriptase (Life Technologies, Carlsbad, CA), 2 mM deoxynucleoside triphosphates, 2.5 mM MgCl$_2$, 1 U RNAsin (all from Applied Biosystems, Foster City, CA), and 0.5 µg of random hexanucleotide primers (Amersham Pharmacia Biotech, Piscataway, NJ). The RT reaction mixture was sequentially incubated at 42°C for 45 min, 52°C for 30 min, and 70°C for 10 min. The reaction was stopped by heating the mixture at 95°C for 5 min. Finally, 0.5 µl of RNase H (Life Technologies, Carlsbad, CA) was added to the RT reaction mixture, which was then incubated at 37°C for 30 min and heat inactivated at 70°C for 10 min, and cDNA pools were stored at −80°C.

Quantitative real-time PCR. Quantitative real-time PCR primers were designed using Primer Express 1.5 (Applied Biosystems, Foster City, CA) and used as previously described (18, 21) on an ABI PRIZM 5700 Sequence Detector (Applied Biosystems, Foster City, CA) using universal cycling conditions (2 min at 50°C and 10 min at 95°C, followed by 40 cycles of 15 s at 95°C and 1 min at 60°C). The cycle threshold (C_T) values were determined by automated analysis. The threshold was set to five times the standard deviation of the nontemplate control. Dissociation curves were recorded after each run, and the amplified products were routinely analyzed by 2% agarose gel electrophoresis.

Raw C_T values were normalized to GAPDH (glyceraldehyde-3-phosphate dehydrogenase) to yield dC_T. The primers in this array had a mean amplification efficiency of 1.9 ± 0.1, which was used to calculate fold induction as 1.9^{ddC_T}. To identify potential deletion in the KSHV genome in long-term-cultured TIVE cells, DNA was extracted and PCR was carried out by using the primers in the KSHV array mentioned above.

Gene expression profiling and data analysis. Total RNA was extracted from TIVE and KSHV-infected TIVE cells at 3 and 10 months postinfection by using Rnazol (Teltest Inc., Friendswood, TX) as recommended by the manufacturer. Gene expression profiling was performed by Case Western Reserve University and the Ireland Cancer Center Gene Expression core facility using Affymetrix technology. All experiments were performed using oligonucleotide-based HG-U95Av2 chips that contained 12,626 probe sets corresponding to human genes and expressed sequence tags. All procedures, starting with the selection of mRNA, reverse transcription, and the generation of biotin-11-CTP- and biotin-16-UTP (Enzo Diagnostics)-labeled cRNA by T7 in vitro transcription, were performed as recommended by Affymetrix and as previously published (3).
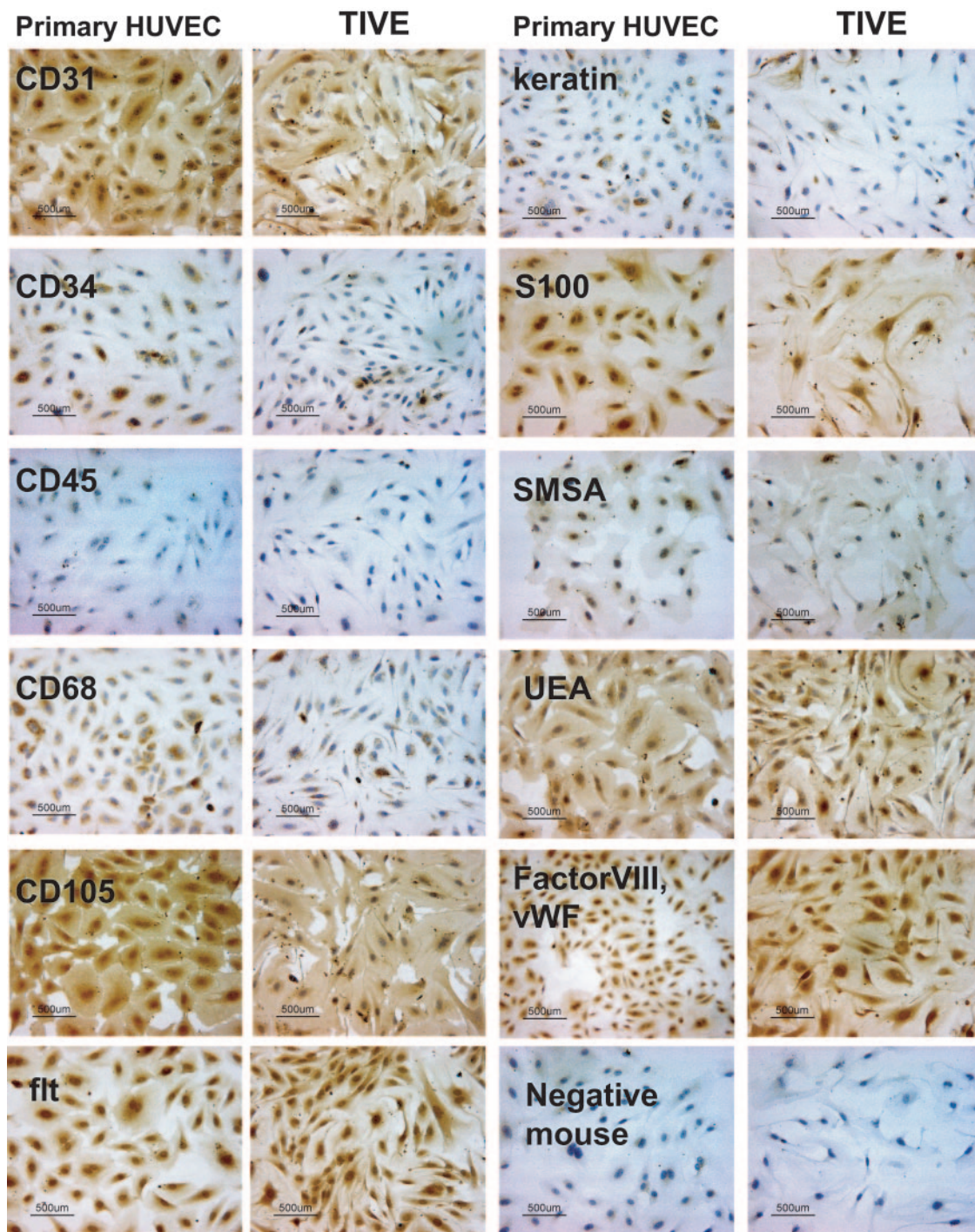
FIG. 1. Immunohistochemical analysis of hTert-immortalized HUVEC in comparison to primary HUVEC; staining for CD31, CD34, CD45, CD68, CD105, Flt, keratin, SMSA, UEA, S100A10, and factor VIII (vWF) expression. The left-hand panels show primary HUVEC at passage 2. The right-hand panels show TIVE cells. TIVE cells strongly express five endothelial-cell-specific markers (CD31, CD105, Flt, UEA, and factor VIII), but not CD45, keratin, or SMSA, which shows slight background staining compared to the primary antibody control (Negative mouse). Note the slightly more elongated morphology of TIVE in contrast to the characteristic cobblestone morphology of HUVEC.

Statistical analysis of data and pairwise comparisons were done using Affymetrix MAS 5.0 software. A detailed description of the analysis was given by An et al. (3), and the original data can be viewed at NCBI gene expression omnibus (GEO).

Statistical analysis. Calculations were performed using Excel (Microsoft Inc., Redwood, WA) and SPSS v. 11.0 (SPSS Science, Chicago, IL). Hierarchical clustering was performed as previously described (3, 50). All samples were normalized to GAPDH, centered by the median of the gene, normalized to ±1, and ordered by hierarchical clustering using ArrayMiner software (Optimal Design Inc., Brussels, Belgium).

Nucleotide sequence accession number. The original data can be viewed at NCBI GEO (accession number GSE1880 [GSM33151, 33152, 33153]).

TABLE 1. Analysis of cell surface markers[a]

Marker	Expression	
	Primary HUVEC (P2)	TIVE cells
CD31	++++	++++
CD34	+	+/−
CD45	−	−
CD68	++	+
CD105	++++	++++
Flt	++++	++++
Keratin	+/−	+/−
SMSA	+/−	+/−
UEA	++++	++++
S100A10	++	++
Factor VIII (vWF)	++++	++++

[a] Endothelium-specific markers are in boldface type. P2, passage 2. + and − indicate relative expression levels.

RESULTS

Establishment of a telomerase-immortalized HUVEC line. Ectopic expression of hTert has been successfully utilized to establish immortalized cell lines of several different lineages (7, 62). Primary umbilical cord-derived HUVEC at passage 2 were transduced with VSV G protein-pseudotyped retrovirus containing either pBabe/hTert or pBabe/GFP packaged in Phoenix cells (kindly provided by G. Nolan, Stanford University). Transduced cells under selection and primary HUVEC were passaged and fed biweekly. After passage 10, both primary HUVEC and pBabe/GFP-transduced cells stopped proliferating. Cells transduced with pBabe/hTert continued to divide. To ensure that endothelial lineage characteristics were maintained after hTert immortalization, a detailed analysis of surface markers was performed. As shown in Fig. 1 and summarized in Table 1, 100% of the cells expressed the endothelial-cell-specific markers CD31, Flt, UEA, CD105, and factor VIII/vWF. CD34, a marker for hematopoietic progenitors and some endothelial cells, which is also expressed in KS tumors, was detectable at low levels in HUVEC at passage 2 and was nearly undetectable in TIVE cells. Expression of CD45, a lymphoid marker, was not detectable, and SMSA, a fibroblastoid marker, showed some background levels. Except for CD34, the observed expression patterns at passage 12 were identical to those of primary umbilical-cord-derived HUVEC at passage 2 (Fig. 1), supporting the notion that hTERT-dependent immortalization does not affect cell lineage commitment. Similar to the previously published TIME cells, which are telomerase-immortalized endothelial cells of dermal microvascular origin (41), we called this cell line TIVE for *t*elomerase-*i*mmortalized *v*ein *e*ndothelial cells. TIVE cells can be propagated once a week at a ratio of 1 to 3 and remain dependent on ECGF. To date, TIVE cells have been cultured continuously for more than 35 passages.

TIVE cells are susceptible to KSHV infection and support lytic replication early after infection. TIVE cells were inoculated with BCBL-1-derived cell-free virus at a multiplicity of infection of 10 (based on genome equivalents) and analyzed by immunofluorescence assays (IFA) for the expression of LANA, a reliable marker for infection (16, 19, 29, 39). Nearly 100% of the cells expressed LANA at 48 h postinfection (Fig. 2A). To confirm

the specificity of the IFA signal, TIVE cells were inoculated with serially diluted cell-free KSHV, and the number of LANA-positive cells decreased accordingly (Fig. 2B). Hence, TIVE cells are susceptible to cell-free KSHV infection.

To determine whether TIVE cells support lytic replication, KSHV-infected cells at 48 h postinfection were either TPA treated or infected with a recombinant adenovirus expressing
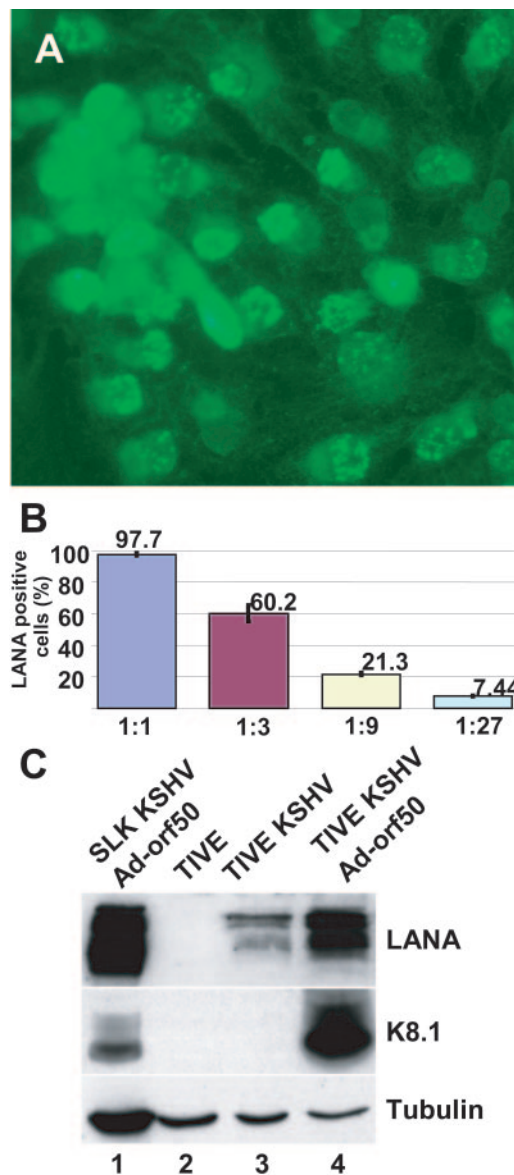

FIG. 2. TIVE cells are susceptible to KSHV and support lytic replication early after infection. (A) LANA IFA on TIVE cells 48 h postinfection with BCBL-1-derived KSHV. (B) Threefold serial dilutions of BCBL-1-derived cell-free virion preparations. The error bars indicate standard deviations. (C) KSHV-infected TIVE cells can be induced to lytic replication. TIVE cells were infected with KSHV or mock infected; 48 h later, the cells were infected with Ad-Orf50, and cell lysates were analyzed by Western blot analysis 72 h later. KSHV-infected SLK cells were used as positive controls. All KSHV-infected SLK cells expressed LANA (lanes 1, 3, and 4). KSHV-infected and -induced TIVE cells expressed significantly more K8.1 than SLK cells. Tubulin was used as a loading control.
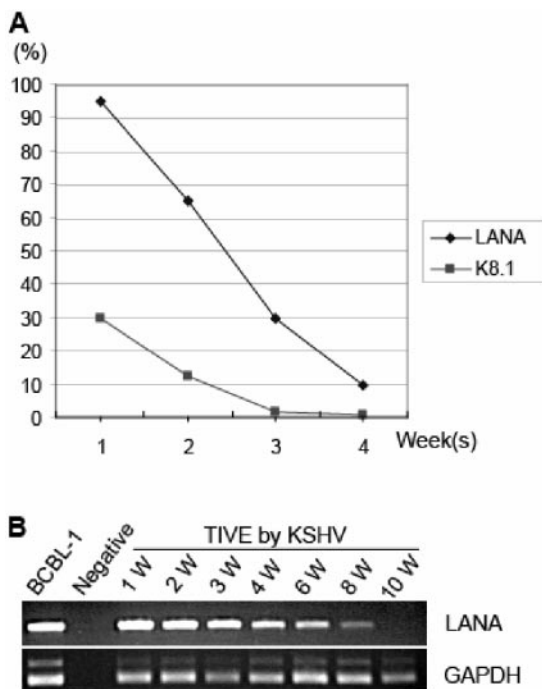
FIG. 3. KSHV-infected TIVE cells lose viral genomes over time. TIVE cells were infected with BCBL-1-derived cell-free KSHV as described in Materials and Methods. At the indicated time points, the cells were analyzed for the expression of LANA and K8.1 and for the presence of viral DNA. (A) IFA for LANA and K8.1. The percentage of LANA-positive cells declined from greater than 95% at week 1 to less than 10% at week 4. A significant percentage of the cells expressed K8.1 at 1 week postinfection; this expression was undetectable at week 4. (B) Detection of viral DNA by PCR. Genomic DNA extracted at the indicated time points was amplified using 25 cycles. The DNA copy number decreased between weeks (W) 4 and 10.

the major lytic transactivator RTA (Ad-Orf50) for 72 h (6, 56). Five days post-KSHV infection, the cells were analyzed for expression of K8.1, a late lytic marker. Characteristic K8.1 staining was observed in about 10% of the cells (data not shown). Western blot analysis showed K8.1 expression that was significantly stronger in infected TIVE cells than in KSHV-infected and -induced SLK cells, which are susceptible to KSHV infection but have been reported to poorly support lytic replication (Fig. 2C) (6). Serial transmission using supernatants from KSHV-infected, TPA-induced TIVE cells to infect naïve TIVE cells was performed three consecutive times and produced LANA-positive cells (see Fig. S1 in the supplemental material). These data show that TIVE cells are susceptible to KSHV, and furthermore, that infected cells can be induced to lytic replication early after infection.

Outgrowth of KSHV-infected TIVE cells that support long-term latency. To determine whether infected TIVE cells could support latency while continuously dividing, we repeat passaged TIVE cells at subconfluency. KSHV-infected TIVE cells (>90% LANA positive) were split 1 to 3 once a week and analyzed for LANA and K8.1 expression. LANA expression decreased to less than 10% at week 4, while K8.1 was undetectable after 4 weeks (Fig. 3A). The percentages of K8.1-expressing cells observed by IFA at 1 week postinfection varied considerably between experiments and may have represented

spontaneously reactivating cells. Using PCR, we observed a steady loss of viral genomes between weeks 4 and 10 postinfection (Fig. 3B). Hence, TIVE cells do not efficiently support latency and long-term episomal maintenance. Similar outcomes were observed in many experiments, and these data are consistent with published observations of KSHV-infected TIME cells, suggesting that long-term maintenance of KSHV in cultured endothelial cells is inefficient (32, 41).

We also observed cases in which TIVE cells remained KSHV positive. As shown in Fig. 4A, after 5 weeks, 8 weeks, and even 10 months, these cells remained 100% LANA positive. LANA expression was confirmed in two cultures by Western blot analysis (Fig. 4B). IFA for both K8.1 and ORF59 were negative; thus, lytic infection was undetectable (data not shown). To further demonstrate latency in contrast to persistence, which requires reinfection, we cultured KSHV-infected TIVE cells for eight passages in the presence of PFA (200 μM), which blocks lytic replication (38). In contrast to prior reports (41), the frequency of LANA-positive cells was not altered in the presence of PFA (Fig. 4C). This demonstrates that in LTC, latent but not lytic replication is sufficient for long-term maintenance of KSHV.

Long-term-infected TIVE cells undergo phenotypic changes reminiscent of transformation. During long-term culture, KSHV-infected TIVE cells underwent notable phenotypic changes. Uninfected TIVE cells grow relatively slowly and are dependent on endothelial-cell growth factors. Initially, KSHV-infected TIVE cells shared these characteristics. However, after 6 to 8 weeks, KSHV-infected cells in two parallel experiments started dividing significantly faster, grew to confluent monolayers, and displayed criss-cross morphology, indicating the loss of contact inhibition. We therefore tested their growth phenotype in soft agar, a widely used assay to assess transformation (17). TIVE or KSHV-infected TIVE cells were seeded into semisolid media and incubated for 14 days. While TIVE cells did not form colonies, KSHV-infected cells at both 3 and 10 months postinfection formed colonies in soft agar (Fig. 5A). To confirm the viability of these cells, we picked 10 colonies and established subclones (LTC 1 to 10). LTC lost their dependence on ECGF, could be split at higher ratios (1 to 10), and had a significantly shorter cell cycle than uninfected TIVE cells, as documented by the much higher proportion of cells in S phase (38% for LTC compared to 10% for TIVE cells) (Fig. 5B). To verify the presence of episomal KSHV DNA in these cells, we performed Gardella gel analysis on five LTC clones. As shown in Fig. 5C, KSHV episomal DNA was readily detectable (8, 18, 60) and migrated at the same position as BCBL-1-derived episomes. This analysis demonstrates the presence of KSHV episomes—however, it does not rule out the presence of integrated KSHV DNA. In sum, LTC represent the first endothelial-cell-derived tumor cell lines in which 100% of the cells are latently infected with KSHV.

LTC express latency-associated genes but do not efficiently reactivate from latency. Next, we examined viral-gene expression during latency and after induction of lytic replication. Genomewide gene expression analysis was performed using a real-time quantitative RT-PCR assay as previously published (18, 21). This assay simultaneously probes for the expression of more than 80 viral genes; three cellular genes are used for normalization. Two LTC clones were analyzed and compared to long-term-infected SLK cells and BCBL-1 cells. Figure 6A
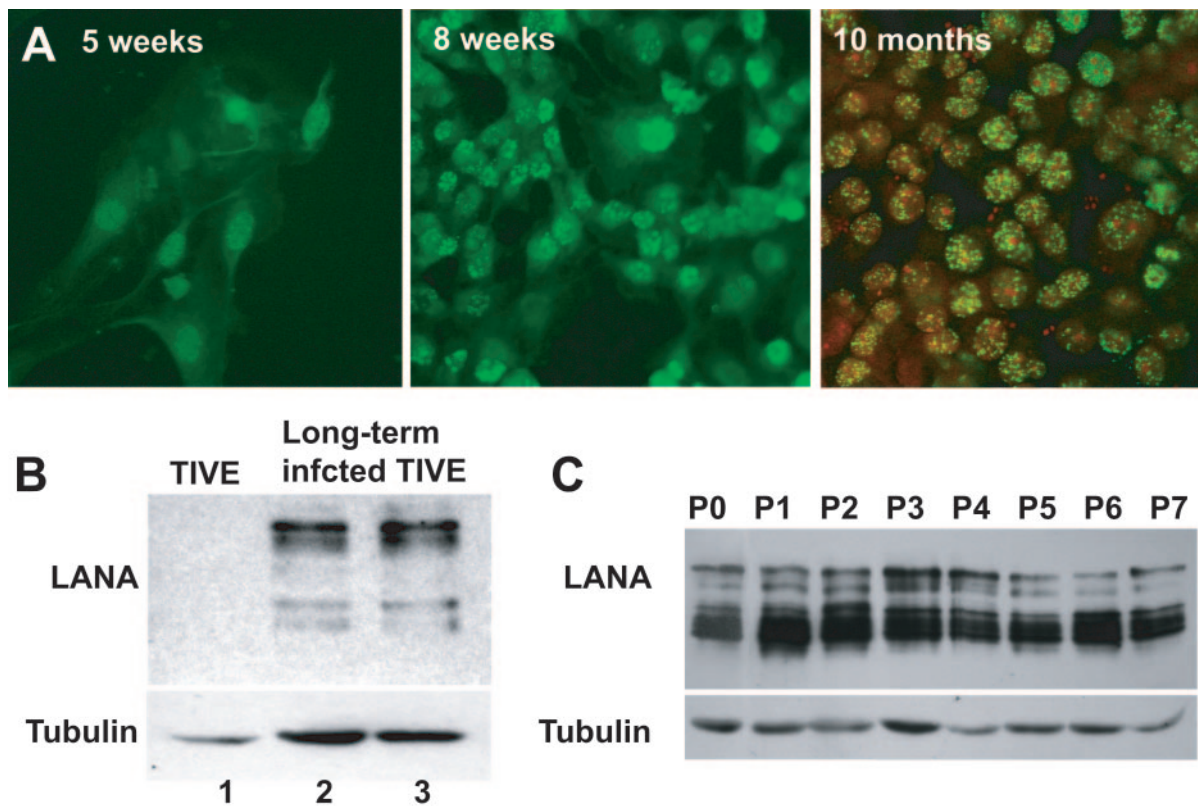
FIG. 4. KSHV-infected TIVE cells support long-term latency. (A) LANA IFA on KSHV-infected TIVE cells 5 and 8 weeks and 10 months postinfection. IFA at 10 months was analyzed by confocal microscopy and double stained with anti-LANA antibodies (green) and propidium iodide (red). (B) LANA detection by Western blot analysis in TIVE cells (lane 1) or KSHV-infected TIVE cells 3 months (lane 2) and 10 months (lane 3) postinfection. (C) Western blot analysis of KSHV-infected TIVE cells that were grown in the presence of 0.5 mM PFA for eight consecutive passages; as a loading control, membranes were stripped and incubated with an α-tubulin-specific antibody (P indicates passage numbers).

shows the viral expression profile from these assays in the form of a heat diagram. LTC and SLK cells express the major latency-associated genes LANA, v-cyclin, and v-Flip, which are expressed from a single genomic locus (16, 58, 63). BCBL-1 cells express the same set of genes, but also some lytic genes, due to a small percentile of spontaneously reactivating cells (12, 56). By comparison, KSHV gene expression in LTC is tightly latent, reminiscent of viral-gene expression in the majority of spindle cells in KS lesions (Fig. 6A, compare lanes 2, 3, and 4) (8, 18, 60).

To analyze and compare gene expression during lytic replication, cultures were either treated with TPA or infected with a recombinant adenovirus expressing the major lytic transactivator RTA (Ad-Orf50) (6) and were analyzed by real-time RT-PCR as described above. Raw data were averaged and normalized to GAPDH (to yield dC_T values). Next, the dC_T for each gene under induced conditions was plotted against the dC_T values under uninduced conditions. Hence, dC_T values that did not change in the presence or absence of induction fell on a diagonal line, while induced genes shifted down.

As expected for BCBL-1 cells, TPA and Ad-Orf50 induced a marked induction of a large number of KSHV genes, indicative of efficient lytic replication (Fig. 6B). In LTC, only Ad-Orf50 infection led to minor expression changes affecting a much smaller number of genes, including orf57, a direct target of Orf50 (Fig. 6C). In contrast, Ad-Orf50 infection of long-

term-infected SLK cells led to a genomewide induction of gene expression (Fig. 6D). These data demonstrate that LTC do not efficiently reactivate from latency.

To confirm these results independently of PCR, we treated LTC with either TPA or Ad-Orf50 and analyzed cell lysates by Western blotting for the expression of K8.1, a late lytic marker. A blot representative of eight total experiments is shown in Fig. 6E. BCBL-1 cells treated for 48 h with TPA or analyzed 5 days post-Ad-Orf50 infection efficiently expressed K8.1 (Fig. 6E, lanes 2 and 3). In contrast, no K8.1 expression was detectable in KSHV-infected TIVE cells after TPA treatment or Ad-Orf50 infection for either 2 or 5 days (Fig. 6E, lanes 4 to 6) under conditions where Ad-GFP infected more than 90% of cells (Fig. 6F). Identical assay conditions efficiently induced lytic replication in TIVE cells and SLK cells 2 days postinfection (Fig. 2C). We note that the assay sensitivity permitted detection of K8.1 in uninduced BCBL-1 cells, with less than 0.5% of cells expressing K8.1 (12).

To rule out any major deletions of the KSHV genome in LTC clones, we extracted genomic DNA and performed genomewide DNA PCR analysis using the primer set described above. We were not able to detect any differences between BCBL-1- and LTC-derived genomes (data not shown). These data demonstrate that latency in long-term-infected TIVE cells is tightly regulated. At this point, we do not know where the block in reactivation lies. The fact that even in the presence of
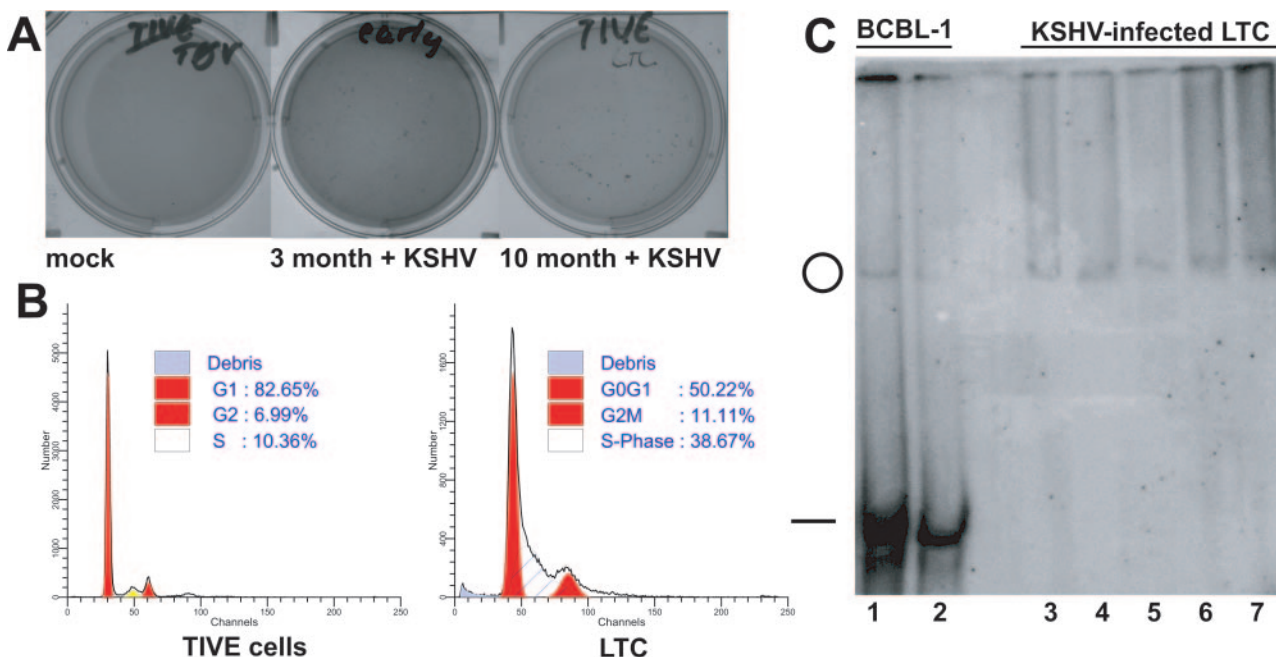
FIG. 5. KSHV-infected TIVE cells display phenotypic changes indicative of transformation. (A) Colony formation assay of TIVE cells or LTC at 3 months and 10 months postinfection; 10,000 cells each were seeded as single-cell suspensions into semisolid media containing EMEM and 5% FCS, and colony growth was scored 2 weeks postinfection. (B) LTC divide faster than TIVE cells. Comparative cell cycle analysis after propidium iodide staining of TIVE cells and LTC. A significantly higher proportion of LTC (39%) than uninfected TIVE cells (10%) were in S phase. (C) Gardella gel analysis of LTC. Five LTC clones established from colonies shown in panel A were analyzed for the presence of episomal KSHV genomes. TPA-induced BCBL-1 cells were loaded as controls to indicate circular and linear genome migration, as previously described (24).

RTA, only a small number of genes, including orf57, were up-regulated suggests epigenetic modifications of the KSHV genome—however, other possibilities cannot be ruled out at this point and will be discussed below.

LTC express many cellular genes that are highly expressed in KS lesions. Next, we analyzed cellular transcriptomes of LTC and TIVE cells. Comparative gene expression profiling was performed on TIVE cells and LTCs at 3 and 10 months postinfection using Affymetrix HG-u95Av2 arrays. RNA extraction, cRNA synthesis, hybridization, washing, and data analysis were performed as previously described (3). All primary data are available at NCBI GEO. Compared to TIVE cells, LTC at 3 or 10 months postinfection showed 1,639 and 1,694 expression changes (>2-fold up or down), of which 869 changes were common to both time points. For the purpose of validating LTC as a model for KS, we focused on two groups of genes. KS lesions are characterized by extensive neoangiogenesis and high levels of cytokine expression (20). In comparison to uninfected TIVE cells, KSHV-positive LTC expressed vascular endothelial growth factor (VEGF) (10- and 13.9-fold), basic fibroblast growth factor (8- and 9.2-fold), and its receptors FGFR1 (2.1- and 2.3-fold) and FGFR4 (6.5- and 4-fold). Interleukin 6 (IL-6), also commonly detected in KS lesions, was induced 2.5-fold in LTC (Table 2).

Since LTC express LANA, we hypothesized that LANA-responsive cellular genes would be induced. LANA regulates viral- and cellular-gene expression in KSHV-associated malignancies. LANA interacts with the tumor suppressors p53 and RB and modulates the Wnt pathway by stabilizing β-catenin. As a result, LANA promotes S-phase entry and protects cells

from apoptosis (24–26, 52). Further supporting these molecular interactions, we recently reported that of a total of 181 gene expression changes observed in LANA-inducible B-cell lines, 41 (23%) were related to RB/E2F signaling (3). Performing a similar analysis on the LTC data set revealed a total of 130 genes (15%) that have been classified as RB/E2F related (45, 49, 53); 19 genes overlapped between LTC and the 41 genes shown to be regulated by LANA. These genes are involved in cell cycle control (CDC25A, cyclin E1, RBP4, and ID1) and DNA synthesis (TTK, TYMS, and DHFR) (Table 2, and NCBI GEO accession number GSE1880). Hence, the overall gene expression profile of LTC at 3 and 10 months postinfection shows a pattern that resembles some important aspects of KS lesions.

Long-term-infected TIVE cells efficiently form tumors in nude mice. Based on the resemblance between KS tumors and LTC (endothelial origin, episomal KSHV maintenance, latent KSHV gene expression, and cellular gene expression profile), we tested LTC in comparison to uninfected TIVE cells for the ability to form tumors in vivo. Nude mice where injected subcutaneously with 5×10^5 TIVE cells in Matrigel as previously described (61). Five mice received LTC at 3 months postinfection, while a second group of five mice received LTC at 10 months postinfection; three mice were injected with uninfected TIVE cells. The animals were visually inspected daily, and the first tumors were palpable around day 7. At day 21 postinoculation, 10/10 mice from both LTC groups had developed tumors approximately 10 to 15 mm in diameter (Fig. 7B and C), while TIVE cell-injected animals did not develop any tumors even after 48 weeks (Fig. 7A). These results are statistically
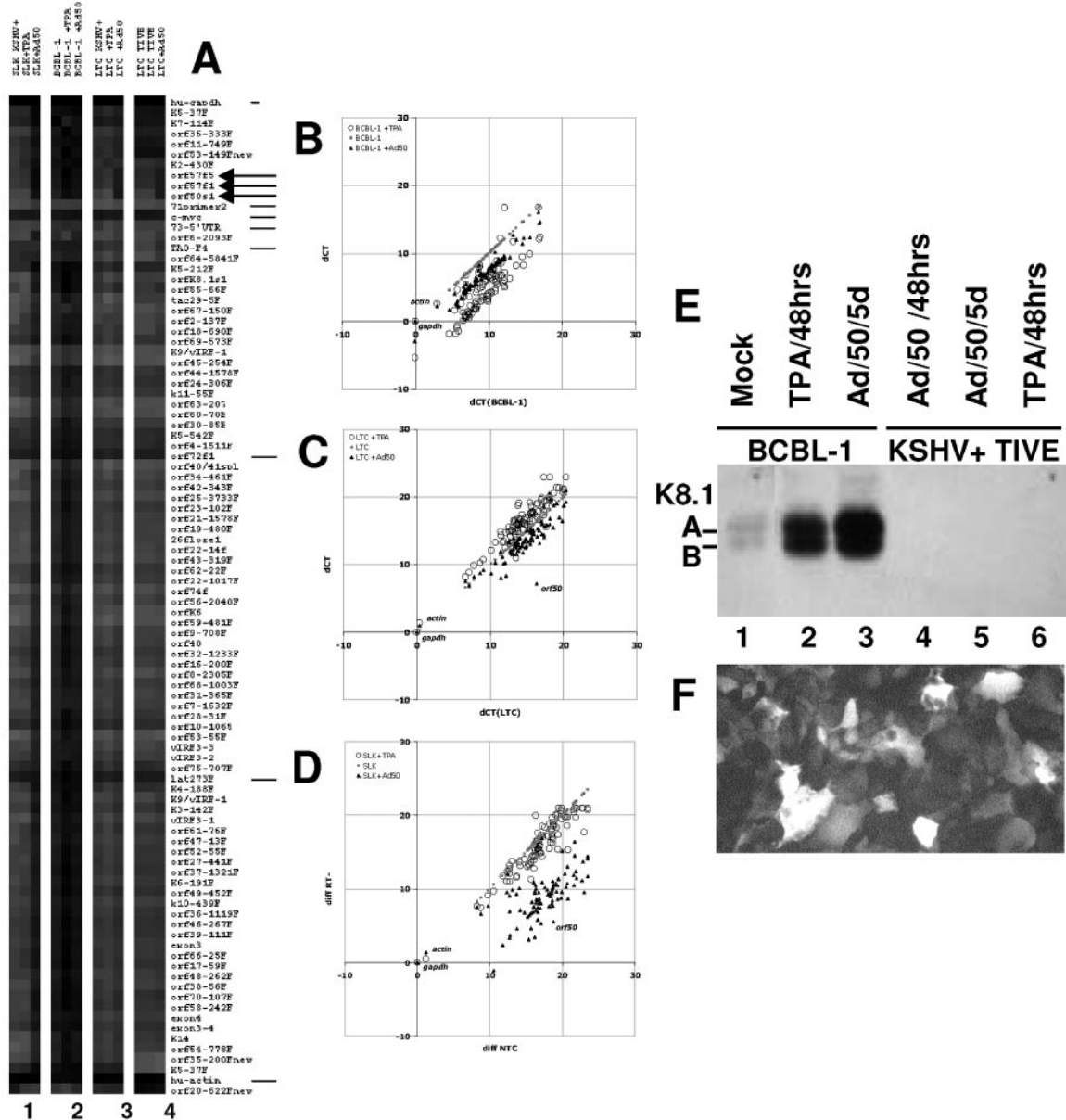
FIG. 6. Comparative genomewide gene expression profiling of LTC and SLK and BCBL-1 cells during latency and after induction of lytic replication; genomewide real-time RT-PCR analysis of LTC-derived tumors. (A) Cluster analysis of multiple experiments, comparing the induction profiles of orf50 and TPA for SLK (lane 1), BCBL-1 (lane 2), and two different LTC (lanes 3 and 4). Each cell line is represented by three columns: uninduced, TPA treated, and Ad-Orf50 infected. The arrows denote the most induced mRNAs, and the bars indicate mRNAs that are not induced. The grayscale indicates the relative level of transcription, normalized to GAPDH. Black indicates the most abundant mRNAs on a $\log_2$ scale. (B, C, and D) Comparative gene expression analysis of BCBL-1 and SLK cells and LTC in response to TPA or Ad-Orf50. The vertical axis indicates dC_T values, normalized to GAPDH, for actin (open triangles), orf50 (open circles), and orf57 (closed squares). A decrease in deltaC_T represents increased levels on a $\log_2$ scale. Panel C plots dC_T values on the vertical axis for mock-treated (gray squares), TPA-treated (open circles), and Ad-Orf50-treated (black triangles) cells relative to mock-treated cells on the horizontal axis for BCBL-1 cells (B), LTC (C), or SLK cells (D). (F) LTC do not efficiently reactivate from latency. Western blot analysis for K8.1 on BCBL-1 cells and long-term-infected LTC clones. LTC clones or BCBL-1 cells as controls were infected with recombinant Ad-Orf50 for 5 days or treated with TPA for 48 h. The cell lysates were tested for K8.1 expression. K8.1 was highly induced in either TPA- or Ad-Orf50-infected cells (lanes 2 and 3). LTC did not express any detectable level of K8.1 (shown is one representative result from a total of eight similar experiments). (E) LTC are susceptible to adenovirus infection. TIVE cells express GFP 48 h postinfection with Ad-GFP.

significant ($P > 0.007$, using nonparametric statistics) and show that LTC, but not TIVE cells, are tumorigenic in mice (Fig. 7D). Mice bearing tumors were sacrificed at day 21, and the tumors were analyzed by histology and immunohistochemistry. Hematoxylin and eosin staining of LTC-induced tumors re-

vealed a mixture of elongated spindle cells and undifferentiated morphology with prominent mitotic figures. In contrast to PEL-derived tumor models (61), there was no well-differentiated layer of cells surrounding the blood vessels. Rather, the tumor cells retained the ability to compose the blood vessel

TABLE 2. Expression changes of cytokine genes and Rb/E2F pathway-related genes in LTC TIVE cells compared to TIVE cells

No.	Access no.[a]	LTC change (n-fold)	Symbol	Gene name
	M83667	2.5	IL-6	Interleukin 6
	AF024710	13.9	VEGF	Vascular endothelial growth factor
	J04513	9.2	bFGF	Basic fibroblast growth factor
1	**U22398**	64	CDKN1C	Cyclin-dependent kinase inhibitor 1C (p57, Kip2)
2	**U69263**	27.9	MATN2	Matrilin 2
3	**X70340**	19.7	TGF-α	Transforming growth factor alpha
4	**M97287**	16	SATB1	Special AT-rich sequence binding protein 1
5	**U30930**	14.9	UGT8	UDP glycosyltransferase 8
6	**U60805**	13.9	OSMR	Oncostatin M receptor
7	**AF053305**	13	BUB1	BUB1 budding uninhibited by benzimidazoles 1 homolog
8	**M34677**	13	F8A1	Coagulation factor VIII-associated (intronic transcript) 1
9	**X15187**	12.1	TRA1	Tumor rejection antigen (gp96) 1
10	J00140	12.1	DHFR	Dihydrofolate reductase, alternate splice 6
11	**U12535**	11.3	EPS8	Epidermal growth factor receptor pathway substrate 8
12	**U81607**	9.2	AKAP12	A kinase (PRKA) anchor protein (gravin) 12
13	**X51345**	8.6	JUNB	*junB* proto-oncogene
14	**M64347**	7	FGFR3	Fibroblast growth factor receptor 3
15	**U61262**	7	NEO1	Neogenin homolog 1 (chicken)
16	**L07540**	6.1	RFC5	Replication factor C (activator 1) 5; 36.5 kDa
17	**X98172**	5.7	CASP8	Caspase 8; apoptosis-related cysteine protease
18	**U59831**	5.7	FOXD1	Forkhead box D1
19	**L37882**	5.7	FZD2	Frizzled homolog 2 (*Drosophila*)
20	U65410	5.7	MAD2L1	MAD2 mitotic arrest deficient-like 1
21	**X84373**	5.7	NRIP1	Nuclear receptor interacting protein 1
22	**U01038**	5.7	PLK1	Polo-like kinase 1 (*Drosophila*)
23	X60673	5.3	AK3L1	Adenylate kinase 3-like 1
24	**AF058696**	5.3	NBS1	Nijmegen breakage syndrome 1 (nibrin)
25	**X89750**	5.3	TGIF	TGF-β-induced factor (TALE family homeobox)
26	S78825	4.9	ID1	Inhibitor of DNA binding 1
27	AF017790	4.9	KNTC2	Kinetochore associated 2
28	**M15205**	4.6	TK1	Thymidine kinase 1; soluble
29	**X76029**	4.3	NMU	Neuromedin U
30	**U89606**	4.3	PDXK	Pyridoxal (pyridoxine; vitamin B_6) kinase
31	M86699	4.3	TTK	TTK protein kinase
32	**U18934**	4.3	TYRO3	TYRO3 protein tyrosine kinase
33	**X51956**	4	ENO2	Enolase 2 (gamma, neuronal)
34	**AB014458**	4	USP1	Ubiquitin-specific protease 1
35	**U18932**	3.7	NDST1	*N*-Deacetylase/*N*-sulfotransferase 1
36	**X06745**	3.7	POLA	Polymerase (DNA directed) alpha
37	M73812	3.5	CCNE1	Cyclin E1
38	X65550	3.5	MKI67	Antigen identified by monoclonal antibody Ki-67
39	**U03911**	3.5	MSH2	*mutS* homolog 2; colon cancer; nonpolyposis type 1
40	**AF029669**	3.5	RAD51C	RAD51 homolog C (*Saccharomyces cerevisiae*)
41	J04088	3.5	TOP2A	Topoisomerase (DNA) II alpha; 170 kDa
42	X02308	3.5	TYMS	Thymidylate synthetase
43	**AJ223728**	3.2	CDC45L	CDC45 cell division cycle 45 like (*S. cerevisiae*)
44	**L19779**	3.2	HIST2H2AA	Histone 2 H2aa
45	**M88108**	3.2	KHDRBS1	KH domain containing; RNA
46	AF030234	3.2	SFRS2IP	Splicing factor: arginine/serine rich 2
47	**U18271**	3.2	TMPO	Thymopoietin
48	**AF049105**	3	CEP2	Centrosomal protein 2
49	**X00088**	3	HIST1H2BJ	Histone 1 H2bj
50	**Z24459**	3	MTCP1	Mature T-cell proliferation 1
51	**U21090**	3	POLD2	Polymerase (DNA directed) delta 2
52	U66618	3	SMARCD2	SWI/SNF related; matrix/actin/chromatin; member 2
53	**Y08837**	3	XRCC2	X-ray repair in Chinese hamster cells 2
54	**X05360**	2.8	CDC2	Cell division cycle 2; G_1 to S and G_2 to M
55	M81933	2.8	CDC25A	Cell division cycle 25A
56	**M63256**	2.8	CDR2	Cerebellar degeneration-related protein 2; 62 kDa
57	**U65093**	2.8	CITED2	Cbp/p300-interacting transactivator, with Glu/Asp-rich c-2
58	**X54942**	2.8	CKS2	CDC28 protein kinase regulatory subunit 2
59	**U61145**	2.8	EZH2	Enhancer of zeste homolog 2 (*Drosophila*)
60	**U75362**	2.8	USP13	Ubiquitin-specific protease 13 (isopeptidase T-3)
61	**Z22535**	2.6	BMPR1A	Bone morphogenetic protein receptor; type IA
62	L41887	2.6	SFRS7	Splicing factor; arginine/serine rich 7; 35 kDa
63	**U61234**	2.6	TBCC	Tubulin-specific chaperone c
64	AB009356	2.5	MAP3K7	Mitogen-activated protein kinase kinase kinase 7

TABLE 2—*Continued*

No.	Access no.[a]	LTC change (*n*-fold)	Symbol	Gene name
65	**D87953**	2.5	NDRG1	N-myc downstream regulated gene 1
66	X74262	2.5	RBBP4	Retinoblastoma binding protein 4
67	**U46751**	2.5	SQSTM1	Sequestosome 1
68	**L36720**	2.3	BYSL	Bystin like
69	**X98743**	2.3	DDX18	DEAD (Asp-Glu-Ala-Asp) box polypeptide 18
70	AF012108	2.3	NCOA3	Nuclear receptor coactivator 3
71	**AB003103**	2.3	PSMD12	Proteasome 26S subunit; non-ATPase; 12
72	**L20859**	2.3	SLC20A1	Solute carrier family 20; member 1
73	**U76366**	2.3	TCOF1	Treacher-Collins-Franceschetti syndrome 1
74	**D89052**	2.1	ATP6V0B	ATPase; H$^+$ transporting; V0 subunit c
75	**M14745**	2.1	BCL2	B-cell CLL/lymphoma 2
76	**U20980**	2.1	CHAF1B	Chromatin assembly factor 1; subunit B (p60)
77	**Z80780**	2.1	HIST1H2BE	Histone 1 H2be
78	**M60725**	2.1	RPS6KB1	Ribosomal protein S6 kinase; 70 kDa; polypeptide 1
79	**AF075587**	2	MYCBP2	MYC binding protein 2
80	**M60858**	2	NCL	Nucleolin
81	**U61232**	2	TBCE	Tubulin-specific chaperone e
82	**U70987**	−2	DOK1	Docking protein 1; 62 kDa
83	**X91648**	−2	PURA	Purine-rich element binding protein A
84	U63824	−2	TEAD4	TEA domain family member 4
85	**M61176**	−2.1	BDNF	Brain-derived neurotrophic factor
86	**L24559**	−2.1	POLA2	Polymerase (DNA directed); alpha 2 (70-kDa subunit)
87	**AF034956**	−2.1	RAD51L3	RAD51-like 3 (*S. cerevisiae*)
88	**L20298**	−2.3	CBFB	Core-binding factor; beta subunit
89	**D38524**	−2.3	NT5C2	5′-nucleotidase, cytosolic II
90	**U43142**	−2.3	VEGFC	Vascular endothelial growth factor C
91	**X58521**	−2.5	NUP62	Nucleoporin; 62 kDa
92	**Z36714**	−2.6	CCNF	Cyclin F
93	**AC004770**	−2.6	FADS3	Fatty acid desaturase 3
94	**D64110**	−2.8	BTG3	BTG family; member 3
95	**AF002668**	−2.8	DEGS1	Degenerative spermatocyte homolog 1; lipid
96	**U76638**	−3	BARD1	BRCA1-associated RING domain 1
97	**L78833**	−3	VAT1	Vesicle amine transport protein 1 homolog (*Torpedo californica*)
98	**X17094**	−3.2	FURIN	Furin (paired basic amino acid-cleaving enzyme)
99	**AF051321**	−3.2	KHDRBS3	KH domain; RNA binding; signal transduction associated 3
100	**U43899**	−3.2	STAM	Signal transducing adaptor molecule (SH3 and ITAM) 1
101	**AF047472**	−3.5	BUB3	BUB3 budding uninhibited by benzimidazoles 3 homolog
102	**D86550**	−3.5	DYRK1A	Dual-specificity tyrosine-(Y)-phosphorylation kinase 1A
103	**J04111**	−3.5	JUN	v-*jun* sarcoma virus 17 oncogene homolog (avian)
104	**U63825**	−4	DIPA	Hepatitis delta antigen-interacting protein A
105	**U63717**	−4.3	OSTF1	Osteoclast-stimulating factor 1
106	**J03764**	−4.3	SERPINE1	Serine (or cysteine) proteinase inhibitor; clade E; member 1
107	**M22490**	−4.6	BMP4	Bone morphogenetic protein 4
108	AF072250	−4.6	MBD4	methyl-CpG binding domain protein 4
109	**J03802**	−4.6	PTHLH	Parathyroid hormone-like hormone
110	**X72889**	−4.6	SMARCA2	SWI/SNF related; matrix/actin/chromatin/member 2
111	**S66431**	−4.9	JARID1A	Jumonji; AT-rich interactive domain 1A (RBBP2-like)
112	**X87843**	−4.9	MNAT1	Ménage à trois 1 (CAK assembly factor)
113	**X15507**	−4.9	Hox5.4	Homeotic protein Hox 5.4
114	**D87119**	−5.7	TRIB2	Tribbles homolog 2 (*Drosophila*)
115	**D87292**	−6.5	TST	Thiosulfate sulfurtransferase (rhodanese)
116	**M85289**	−8.6	HSPG2	Heparan sulfate proteoglycan 2 (perlecan)
117	**M31166**	−12.1	PTX3	Pentraxin-related gene,; rapidly induced by IL-1β
118	**U16954**	−14.9	AF1Q	ALL1-fused gene from chromosome 1q
119	**X03473**	−17.1	H1F0	H1 histone family; member 0
120	**U67784**	−18.4	CMKOR1	Chemokine orphan receptor 1
121	**M64497**	−18.4	NR2F2	Nuclear receptor subfamily 2; group F; member 2
122	**J02854**	−22.6	MYL9	Myosin; light polypeptide 9; regulatory
123	**U68723**	−29.9	CHES1	Checkpoint suppressor 1
124	**Z37976**	−68.6	LTBP2	Latent transforming growth factor beta binding protein 2
125	**X52947**	−78.8	GJA1	Gap junction protein alpha 1; 43 kDa (connexin 43)
126	**M22489**	−104	BMP2	Bone morphogenetic protein 2
127	**X93510**	−119.4	PDLIM4	PDZ and LIM domain 4
128	**X82209**	−128	MN1	Meningioma (disrupted in balanced translocation) 1
129	**L27560**	−207.9	IGFBP5	Insulin-like growth factor binding protein 5
130	**U03877**	−256	EFEMP1	EGF-containing fibulin-like extracellular matrix protein 1

[a] Boldface genes were also found to be changed in B lymphocytes expressing LANA in an inducible fashion (3); the full data set can be found at NCBI GEO (accession no. GSE1880).
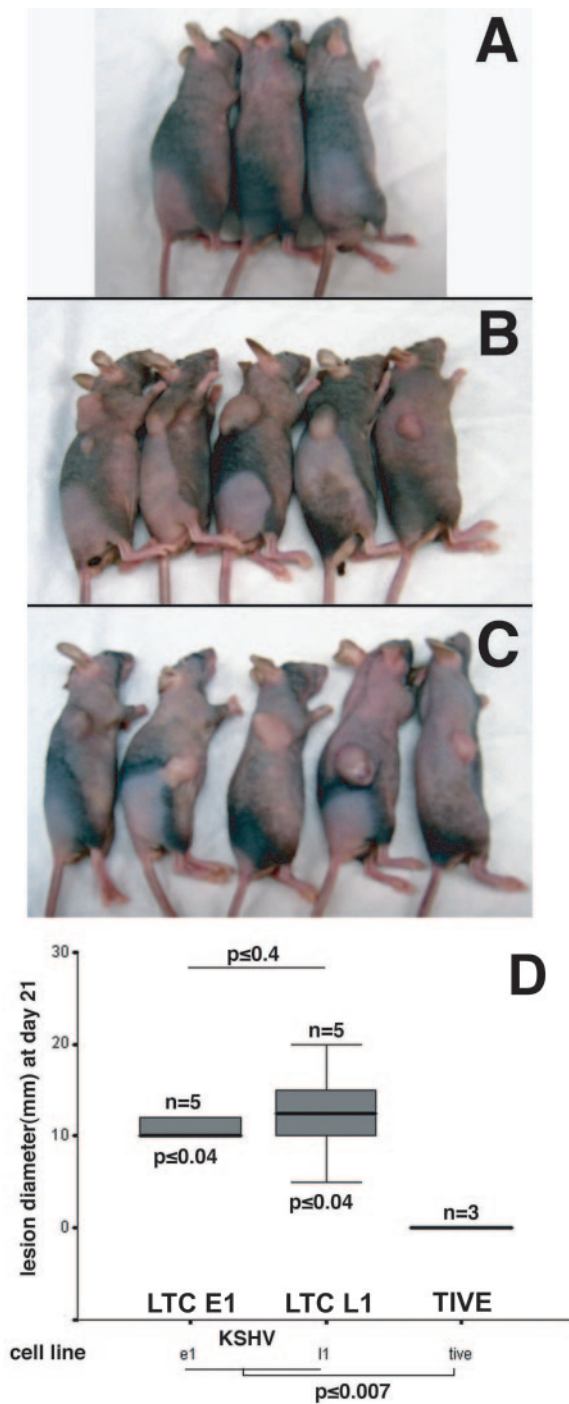
FIG. 7. LTC are highly tumorigenic in NUDE mice. Uninfected TIVE cells or LTC (10^5 cells in growth factor-depleted Matrigel) established at 3 or 10 months postinfection were injected subcutaneously into nude mice. (A, B, and C) Mice injected with LTC at 3 (5/5) and 10 (5/5) months developed tumors, while none of the control mice injected with TIVE cells (0/3) did. (D) Graph indicating the size and distribution of resulting tumors. Pairwise comparisons using sum-rank statistics demonstrate statistical significance. Boxes represent interquartile ranges; lines within boxes represent the medians; T bars indicate highest and lowest observed values.
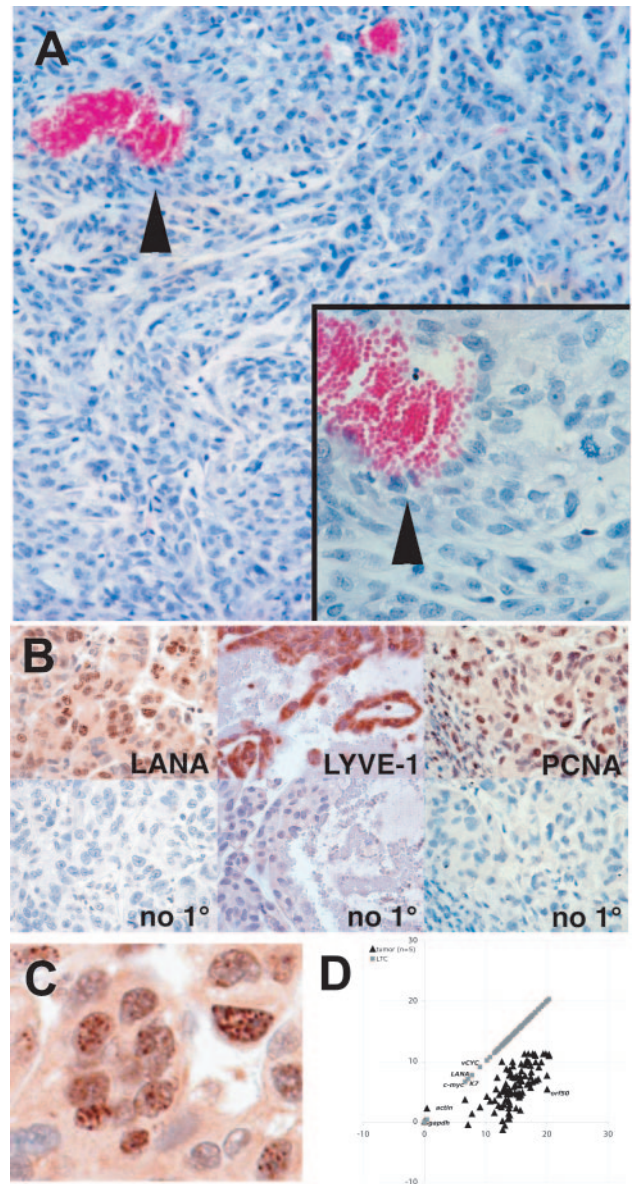

FIG. 8. LTC-derived tumor cells express LANA and LYVE-1 and show a more permissive viral expression pattern than LTC grown in vitro. LTC-derived tumors were dissected and analyzed for protein and viral-mRNA expression. (A) Hematoxylin and eosin staining of L1 tumor displaying a mixture of elongated-spindle-cell and undifferentiated morphologies with prominent mitotic figures. The inset shows tumor cells closely surrounding a blood vessel. The arrowheads indicate erythrocytes extravasated into the tumor. (B and C) Immunohistochemical detection of LANA, LYVE-1, and PCNA. Shown is one representative panel out of five tumor samples. Panel C shows an enlarged tissue section from panel B to emphasize typical LANA speckled staining. (D) Genomewide real-time RT-PCR analysis of LTC-derived tumors. The graph shows mean expression levels from pooled mRNA samples taken from a total of five LTC-derived tumors (two at 3 months and 3 at 10 months postinfection). The data are plotted as dC_T in comparison to GAPDH and LTC. A much broader gene expression pattern in tumors than in LTC grown in vitro is shown.

lining, and erythrocytes extravasated into the tumor (Fig. 8A). Importantly, every cell in these tumors expressed the characteristic nuclear speckled pattern for LANA (Fig. 8B and C). KSHV infection of primary HUVEC cells induced differenti-

ation into the lymphatic endothelium, for which LYVE-1 is a marker (10, 34, 64). LYVE-1 is also expressed on KS spindle cells. To test the hypothesis that LTC maintained this phenotype, we stained tumor sections with antibodies for LYVE-1. We also stained the tumor sections with PCNA, which is a marker for proliferating cells. The majority of cells stained positive for both antigens, suggesting that LTC-induced tumors display features of KS lesions (Fig. 8B).

LTC-derived tumors express both latent and lytic genes. Within KS lesions, the majority of cells are latently infected. However, a small number of cells in each tumor also express lytic markers, and the proportions of lytic-gene expression vary between KS biopsies (8, 18, 60). This maybe important for pathogenesis, since many potential KSHV-encoded pathogenesis modifiers (i.e., vGPCR, K1, K3, and K5) are not expressed during latency in PEL (14, 36, 40, 42). Therefore, a model has been proposed in which a relatively small number of cells reactivate and actively contribute to tumor homeostasis through paracrine effects (4, 32). At this point, it is unresolved whether these cells actively replicate virus or simply show a more extensive pattern of early gene expression. To determine viral-gene expression in LTC-derived tumors, we analyzed five dissected LTC-derived tumors by genomewide quantitative real-time RT-PCR. Figure 8D shows the mean expression level ($n = 5$) of KSHV mRNAs relative to GAPDH mRNA levels and in comparison to LTC that were cultivated in vitro. In tumors, about 25% of all KSHV mRNAs were present at 10% of GAPDH mRNA levels. The mRNAs for orf55, orf17, orf4, gM, helicase, and K7 were present at or above the level of LANA mRNA (Fig. 8D). These observations were in stark contrast to the tightly regulated latent gene regulation observed in LTC when cultured in vitro (Fig. 6). Hence, in vivo growth of KSHV-infected LTC is associated with a more permissive viral transcription pattern. A similar phenotype was reported when latently infected PEL cells were transplanted into mice (61). In summary, these data demonstrate that in vitro-infected LTC, when introduced into mice, generate a tumor that recapitulates hallmark features of KS lesions. To date, LTC represents the first and only xenograft model for KS tumors based on in vitro-infected human endothelial cells.

DISCUSSION

TIVE cells provide a novel cell type in which to study KSHV biology. As demonstrated by cell surface marker expression, TIVE cells preserved a typical endothelial phenotype after transduction with hTert (Fig. 1 and Table 1). Consistent with previous reports demonstrating that hTert expression alone does not lead to alterations in p53 and/or Rb pathways, TIVE cells did not grow in soft agar or form tumors in mice (Fig. 5 and 7) (47). Like primary endothelial cells (HUVEC) or immortalized endothelial cells, TIVE cell cultures are susceptible to cell-free KSHV infection and support lytic replication early after infection (Fig. 2). Phenotypically, early TIVE cell passages more closely resemble primary HUVEC than either TIME cells (41) or E6/E7-immortalized HUVEC, in which many pathways targeted by latency-associated genes are deregulated prior to infection with KSHV (24, 26, 48, 52). TIVE cells complement these existing models and are useful to study aspects of latent and lytic replication early after infection. Like other endothelial-cell cul-

ture systems, TIVE cells infected with KSHV lose the viral genome over time (32) (Fig. 3). However, the outgrowth of two KSHV long-term-infected TIVE cell lines provide for the first time the opportunity to study latency in endothelial cells that support long-term episomal maintenance. The growth phenotypes of these two cell lines in soft agar allowed us to establish 10 LTC clones, which remained 100% KSHV infected (Fig. 4 and 5). Hence, in the TIVE model, maintenance of the viral episome is a clonal, cell-autonomous phenotype. The frequency of this event is low, which is consistent with cellular transformation and can be rationalized analogously to the emergence of androgen-independent clones in early-stage prostate cancer cell lines. Preliminary data from transfecting LANA-specific small interfering RNA constructs into LTC suggested that, as recently demonstrated for PEL cells (15, 31), latent KSHV gene expression may also directly contribute to the survival of LTC (R. Renne, unpublished data). Therefore, further development of TIVE-like cell lines may ultimately be useful to determine KSHV genes whose expression contributes to tumorigenesis in the context of the intact viral genome, comparable to the outgrowth of lymphoblastoid cell lines in response to Epstein-Barr virus infection of human B cells (44).

In contrast to previously described DMVEC-based models, LTC do not reactivate spontaneously from latency. Indeed, even the expression of Ad-Orf50 did not induce efficient lytic replication (Fig. 6). However, in vitro-cultured LTC expressed the major latency-associated genes of KSHV that are highly expressed in KS lesions. Once introduced into mice, the resulting tumors showed a more permissive gene expression profile reminiscent of a minority of cells within KS lesions (8, 60) (Fig. 8). Our preliminary gene expression profiling data revealed a large number of cellular genes whose expression was associated with KS tumors (e.g., VEGF, basic fibroblast growth factor, and IL-6) (Table 2). Therefore, a more detailed expression analysis of LTC in comparison to LTC tumors will provide insights into the cellular-gene expression profile of KS cells. So far, cellular-gene expression studies with KSHV-infected cells have used either PEL-derived cell lines, de novo-infected endothelial-cell lines, or primary cells that represent a mixture of latently and lytically infected cells (3, 13, 22, 37).

Many lines of evidence point to LANA, v-cyclin, and v-Flip as essential players in KS pathogenesis. LANA, like simian virus 40 large T antigen, is a replication/transcription factor that modulates the major tumor suppressors p53 and RB (5, 24, 35, 52). Recently, LANA has also been shown to directly affect the Wnt/β-catenin signaling pathway in lymphomas, which is altered in many human malignancies (25, 26). In this context, it is important that TIVE cells have not been immortalized by viral oncogenes, such as E6/E7, that prevent studies of the above-mentioned signaling pathways. Hence, TIVE cells early after infection with KSHV and long-term-infected LTC provide a cell culture model in which to study latency and its potential role in KSHV-dependent tumorigenesis.

Until now, all reported KSHV tumor models have utilized PEL-derived cell lines or cells transfected with individual KSHV ORFs encoding potential oncogenes (4, 28, 46). This is largely due to the lack of endothelial cells that stably maintained KSHV after in vitro infection. However, PEL lymphomagenesis, which is closely tied to B-cell maturation in germinal centers, differs from the development of KS disease

(22, 37). Hence, the generation of stably infected LTC and the fact that LTC (10/10) but not TIVE cells (0/3) efficiently formed tumors in nude mice represent the first xenograft model for KS. Moreover, the analysis of LTC-derived tumors revealed many features observed in KS lesions, including the expression of LYVE and angiogenic cytokines, such as VEGF and IL-6 (Fig. 7 and 8). LTC-derived tumors recapitulate many virological and cellular characteristics of KS tumors; therefore, newly developed and existing drugs could be tested for efficacy to inhibit tumor growth in this model.

Very recently, several groups have reported on the identification of KSHV-encoded microRNAs (miRNAs) within the latency-associated region of KSHV (9, 51, 57). miRNAs posttranscriptionally modulate cellular- and/or viral-gene expression and might represent a new class of viral genes that contribute to pathogenesis. KSHV-encoded miRNAs are transcribed in LTC and LTC-derived tumors at a level comparable to those of other mRNAs in the LANA latency cluster (D. P. Dittmer and R. Renne, unpublished data) and will provide a unique opportunity to functionally analyze miRNA expression during latent and lytic replication in vivo (57).

Finally, this model will aid studies of the contributions of latent and lytic genes to KSHV-dependent pathogenesis and tumorigenesis in vivo. Within this context, we found viral-gene expression to be much more permissive in LTC-derived tumors (Fig. 8D) than in LTC grown in vitro (Fig. 6C). These observations are in agreement with gene expression in KS tumors, as well as with previous observations on PEL-derived tumor models (61), and suggest that the tumor microenvironment is crucial in modeling host-viral interactions as present in KS disease.

ACKNOWLEDGMENTS

REFERENCES

1. **Ablashi, D. V., L. G. Chatlynne, J. E. Whitman, Jr., and E. Cesarman.** 2002. Spectrum of Kaposi's sarcoma-associated herpesvirus, or human herpesvirus 8, diseases. Clin. Microbiol. Rev. **15:**439–464.
2. **Aluigi, M. G., A. Albini, S. Carlone, L. Repetto, R. De Marchi, A. Icardi, M. Moro, D. Noonan, and R. Benelli.** 1996. KSHV sequences in biopsies and cultured spindle cells of epidemic, iatrogenic and Mediterranean forms of Kaposi's sarcoma. Res. Virol. **147:**267–275.
3. **An, F. Q., N. Compitello, E. Horwitz, M. Sramkoski, E. S. Knudsen, and R. Renne.** 2005. The latency-associated nuclear antigen of Kaposi's sarcoma-associated herpesvirus modulates cellular gene expression and protects lymphoid cells from p16 INK4A-induced cell cycle arrest. J. Biol. Chem. **280:**3862–3874.
4. **Bais, C., B. Santomasso, O. Coso, L. Arvanitakis, E. G. Raaka, J. S. Gutkind, A. S. Asch, E. Cesarman, E. A. Mesri, and M. C. Gershengorn.** 1998. G-protein-coupled receptor of Kaposi's sarcoma-associated herpesvirus is a viral oncogene and angiogenesis activator. Nature **391:**86–89.
5. **Ballestas, M. E., P. A. Chatis, and K. M. Kaye.** 1999. Efficient persistence of extrachromosomal KSHV DNA mediated by latency-associated nuclear antigen. Science **284:**641–644.
6. **Bechtel, J. T., Y. Liang, J. Hvidding, and D. Ganem.** 2003. Host range of Kaposi's sarcoma-associated herpesvirus in cultured cells. J. Virol. **77:**6474–6481.
7. **Blackburn, E. H.** 2000. Telomere states and cell fates. Nature **408:**53–56.
8. **Boshoff, C., T. F. Schulz, M. M. Kennedy, A. K. Graham, C. Fisher, A. Thomas, J. O. McGee, R. A. Weiss, and J. J. O'Leary.** 1995. Kaposi's sarcoma-associated herpesvirus infects endothelial and spindle cells. Nat. Med. **1:**1274–1278.
9. **Cai, X., S. Lu, Z. Zhang, C. M. Gonzalez, B. Damania, and B. R. Cullen.** 2005. Kaposi's sarcoma-associated herpesvirus expresses an array of viral microRNAs in latently infected cells. Proc. Natl. Acad. Sci. USA **102:**5570–5575.
10. **Carroll, P. A., E. Brazeau, and M. Lagunoff.** 2004. Kaposi's sarcoma-associated herpesvirus infection of blood endothelial cells induces lymphatic differentiation. Virology **328:**7–18.
11. **Cesarman, E., Y. Chang, P. S. Moore, J. W. Said, and D. M. Knowles.** 1995. Kaposi's sarcoma-associated herpesvirus-like DNA sequences in AIDS-related body-cavity-based lymphomas. N. Engl. J. Med. **332:**1186–1191.
12. **Chang, J., R. Renne, D. Dittmer, and D. Ganem.** 2000. Inflammatory cytokines and the reactivation of Kaposi's sarcoma-associated herpesvirus lytic replication. Virology **266:**17–25.
13. **Ciufo, D. M., J. S. Cannon, L. J. Poole, F. Y. Wu, P. Murray, R. F. Ambinder, and G. S. Hayward.** 2001. Spindle cell conversion by Kaposi's sarcoma-associated herpesvirus: formation of colonies and plaques with mixed lytic and latent gene expression in infected primary dermal microvascular endothelial cell cultures. J. Virol. **75:**5614–5626.
14. **Coscoy, L., and D. Ganem.** 2000. Kaposi's sarcoma-associated herpesvirus encodes two proteins that block cell surface display of MHC class I chains by enhancing their endocytosis. Proc. Natl. Acad. Sci. USA **97:**8051–8056.
15. **Curreli, F., A. E. Friedman-Kien, and O. Flore.** 2005. Glycyrrhizic acid alters Kaposi sarcoma-associated herpesvirus latency, triggering p53-mediated apoptosis in transformed B lymphocytes. J. Clin. Investig. **115:**642–652.
16. **Dittmer, D., M. Lagunoff, R. Renne, K. Staskus, A. Haase, and D. Ganem.** 1998. A cluster of latently expressed genes in Kaposi's sarcoma-associated herpesvirus. J. Virol. **72:**8309–8315.
17. **Dittmer, D., S. Pati, G. Zambetti, S. Chu, A. K. Teresky, M. Moore, C. Finlay, and A. J. Levine.** 1993. Gain of function mutations in p53. Nat. Genet. **4:**42–46.
18. **Dittmer, D. P.** 2003. Transcription profile of Kaposi's sarcoma-associated herpesvirus in primary Kaposi's sarcoma lesions as determined by real-time PCR arrays. Cancer Res. **63:**2010–2015.
19. **Dupin, N., C. Fisher, P. Kellam, S. Ariad, M. Tulliez, N. Franck, E. van Marck, D. Salmon, I. Gorin, J. P. Escande, R. A. Weiss, K. Alitalo, and C. Boshoff.** 1999. Distribution of human herpesvirus-8 latently infected cells in Kaposi's sarcoma, multicentric Castleman's disease, and primary effusion lymphoma. Proc. Natl. Acad. Sci. USA **96:**4546–4551.
20. **Ensoli, B., M. Sturzl, and P. Monini.** 2001. Reactivation and role of HHV-8 in Kaposi's sarcoma initiation. Adv. Cancer Res. **81:**161–200.
21. **Fakhari, F. D., and D. P. Dittmer.** 2002. Charting latency transcripts in Kaposi's sarcoma-associated herpesvirus by whole-genome real-time quantitative PCR. J. Virol. **76:**6213–6223.
22. **Fan, W., D. Bubman, A. Chadburn, W. J. Harrington, Jr., E. Cesarman, and D. M. Knowles.** 2005. Distinct subsets of primary effusion lymphoma can be identified based on their cellular gene expression profile and viral association. J. Virol. **79:**1244–1251.
23. **Flore, O., S. Rafii, S. Ely, J. J. O'Leary, E. M. Hyjek, and E. Cesarman.** 1998. Transformation of primary human endothelial cells by Kaposi's sarcoma-associated herpesvirus. Nature **394:**588–592.
24. **Friborg, J., Jr., W. Kong, M. O. Hottiger, and G. J. Nabel.** 1999. p53 inhibition by the LANA protein of KSHV protects against cell death. Nature **402:**889–894.
25. **Fujimuro, M., and S. D. Hayward.** 2003. The latency-associated nuclear antigen of Kaposi's sarcoma-associated herpesvirus manipulates the activity of glycogen synthase kinase-3β. J. Virol. **77:**8019–8030.
26. **Fujimuro, M., F. Y. Wu, C. ApRhys, H. Kajumbula, D. B. Young, G. S. Hayward, and S. D. Hayward.** 2003. A novel viral mechanism for dysregulation of beta-catenin in Kaposi's sarcoma-associated herpesvirus latency. Nat. Med. **9:**300–306.
27. **Ganem, D.** 1997. KSHV and Kaposi's sarcoma: the end of the beginning? Cell **91:**157–160.
28. **Gao, S. J., C. Boshoff, S. Jayachandra, R. A. Weiss, Y. Chang, and P. S. Moore.** 1997. KSHV ORF K9 (vIRF) is an oncogene which inhibits the interferon signaling pathway. Oncogene **15:**1979–1985.
29. **Gao, S. J., L. Kingsley, M. Li, W. Zheng, C. Parravicini, J. Ziegler, R. Newton, C. R. Rinaldo, A. Saah, J. Phair, R. Detels, Y. Chang, and P. S. Moore.** 1996. KSHV antibodies among Americans, Italians and Ugandans with and without Kaposi's sarcoma. Nat. Med. **2:**925–928.
30. **Gimbrone, M. A., Jr.** 1976. Culture of vascular endothelium. Prog. Hemost. Thromb. **3:**1–28.
31. **Godfrey, A., J. Anderson, A. Papanastasiou, Y. Takeuchi, and C. Boshoff.** 2005. Inhibiting primary effusion lymphoma by lentiviral vectors encoding short hairpin RNA. Blood **105:**2510–2518.
32. **Grundhoff, A., and D. Ganem.** 2004. Inefficient establishment of KSHV latency suggests an additional role for continued lytic replication in Kaposi sarcoma pathogenesis. J. Clin. Investig. **113:**124–136.

33. **Guasparri, I., S. A. Keller, and E. Cesarman.** 2004. KSHV vFLIP is essential for the survival of infected lymphoma cells. J. Exp. Med. **199:**993–1003.

34. **Hong, Y. K., K. Foreman, J. W. Shin, S. Hirakawa, C. L. Curry, D. R. Sage, T. Libermann, B. J. Dezube, J. D. Fingeroth, and M. Detmar.** 2004. Lymphatic reprogramming of blood vascular endothelium by Kaposi sarcoma-associated herpesvirus. Nat. Genet. **36:**683–685.

35. **Hu, J., A. C. Garber, and R. Renne.** 2002. The latency-associated nuclear antigen of Kaposi's sarcoma-associated herpesvirus supports latent DNA replication in dividing cells. J. Virol. **76:**11677–11687.

36. **Ishido, S., C. Wang, B. S. Lee, G. B. Cohen, and J. U. Jung.** 2000. Down-regulation of major histocompatibility complex class I molecules by Kaposi's sarcoma-associated herpesvirus K3 and K5 proteins. J. Virol. **74:**5300–5309.

37. **Jenner, R. G., K. Maillard, N. Cattini, R. A. Weiss, C. Boshoff, R. Wooster, and P. Kellam.** 2003. Kaposi's sarcoma-associated herpesvirus-infected primary effusion lymphoma has a plasma cell gene expression profile. Proc. Natl. Acad. Sci. USA **100:**10399–10404.

38. **Kedes, D. H., and D. Ganem.** 1997. Sensitivity of Kaposi's sarcoma-associated herpesvirus replication to antiviral drugs. Implications for potential therapy. J. Clin. Investig. **99:**2082–2086.

39. **Kedes, D. H., E. Operskalski, M. Busch, R. Kohn, J. Flood, and D. Ganem.** 1996. The seroepidemiology of human herpesvirus 8 (Kaposi's sarcoma-associated herpesvirus): distribution of infection in KS risk groups and evidence for sexual transmission Nat. Med. **2:**918–924. [Erratum, **2:**1041.]

40. **Kirshner, J. R., K. Staskus, A. Haase, M. Lagunoff, and D. Ganem.** 1999. Expression of the open reading frame 74 (G-protein-coupled receptor) gene of Kaposi's sarcoma (KS)-associated herpesvirus: implications for KS pathogenesis. J. Virol. **73:**6006–6014.

41. **Lagunoff, M., J. Bechtel, E. Venetsanakos, A. M. Roy, N. Abbey, B. Herndier, M. McMahon, and D. Ganem.** 2002. De novo infection and serial transmission of Kaposi's sarcoma-associated herpesvirus in cultured endothelial cells. J. Virol. **76:**2440–2448.

42. **Lagunoff, M., D. M. Lukac, and D. Ganem.** 2001. Immunoreceptor tyrosine-based activation motif-dependent signaling by Kaposi's sarcoma-associated herpesvirus K1 protein: effects on lytic viral replication. J. Virol. **75:**5891–5898.

43. **Lebbe, C., P. de Cremoux, G. Millot, M. P. Podgorniak, O. Verola, R. Berger, P. Morel, and F. Calvo.** 1997. Characterization of in vitro culture of HIV-negative Kaposi's sarcoma-derived cells. In vitro responses to alfa interferon. Arch. Dermatol. Res. **289:**421–428.

44. **Liebowitz, D., and E. Kieff.** 1993. Epstein-Barr virus, p. 107–172. *In* B. Roizman, R. J. Whitley, and C. Lopez (ed.), The human herpesviruses. Raven Press, New York, N.Y.

45. **Markey, M. P., S. P. Angus, M. W. Strobeck, S. L. Williams, R. W. Gunawardena, B. J. Aronow, and E. S. Knudsen.** 2002. Unbiased analysis of RB-mediated transcriptional repression identifies novel targets and distinctions from E2F action. Cancer. Res. **62:**6587–6597.

46. **Montaner, S., A. Sodhi, A. Molinolo, T. H. Bugge, E. T. Sawai, Y. He, Y. Li, P. E. Ray, and J. S. Gutkind.** 2003. Endothelial infection with KSHV genes in vivo reveals that vGPCR initiates Kaposi's sarcomagenesis and can promote the tumorigenic potential of viral latent genes. Cancer Cell **3:**23–36.

47. **Morales, C. P., S. E. Holt, M. Ouellette, K. J. Kaur, Y. Yan, K. S. Wilson, M. A. White, W. E. Wright, and J. W. Shay.** 1999. Absence of cancer-associated changes in human fibroblasts immortalized with telomerase. Nat. Genet. **21:**115–118.

48. **Moses, A. V., K. N. Fish, R. Ruhl, P. P. Smith, J. G. Strussenberg, L. Zhu, B. Chandran, and J. A. Nelson.** 1999. Long-term infection and transformation of dermal microvascular endothelial cells by human herpesvirus 8. J. Virol. **73:**6892–6902.

49. **Muller, H., A. P. Bracken, R. Vernell, M. C. Moroni, F. Christians, E. Grassilli, E. Prosperini, E. Vigo, J. D. Oliner, and K. Helin.** 2001. E2Fs regulate the expression of genes involved in differentiation, development, proliferation, and apoptosis. Genes Dev. **15:**267–285.

50. **Papin, J., W. Vahrson, R. Hines-Boykin, and D. P. Dittmer.** 2005. Real-time quantitative PCR analysis of viral transcription. Methods Mol. Biol. **292:**449–480.

51. **Pfeffer, S., A. Sewer, M. Lagos-Quintana, R. Sheridan, C. Sander, F. A. Grasser, L. F. van Dyk, C. K. Ho, S. Shuman, M. Chien, J. J. Russo, J. Ju, G. Randall, B. D. Lindenbach, C. M. Rice, V. Simon, D. D. Ho, M. Zavolan, and T. Tuschl.** 2005. Identification of microRNAs of the herpesvirus family. Nat. Methods **2:**269–276.

52. **Radkov, S. A., P. Kellam, and C. Boshoff.** 2000. The latent nuclear antigen of Kaposi sarcoma-associated herpesvirus targets the retinoblastoma-E2F pathway and with the oncogene Hras transforms primary rat cells. Nat. Med. **6:**1121–1127.

53. **Ren, B., H. Cam, Y. Takahashi, T. Volkert, J. Terragni, R. A. Young, and B. D. Dynlacht.** 2002. E2F integrates cell cycle progression with DNA repair, replication, and G_2/M checkpoints. Genes Dev. **16:**245–256.

54. **Renne, R., D. Blackbourn, D. Whitby, J. Levy, and D. Ganem.** 1998. Limited transmission of Kaposi's sarcoma-associated herpesvirus in cultured cells. J. Virol. **72:**5182–5188.

55. **Renne, R., M. Lagunoff, W. Zhong, and D. Ganem.** 1996. The size and conformation of Kaposi's sarcoma-associated herpesvirus (human herpesvirus 8) DNA in infected cells and virions. J. Virol. **70:**8151–8154.

56. **Renne, R., W. Zhong, B. Herndier, M. McGrath, N. Abbey, D. Kedes, and D. Ganem.** 1996. Lytic growth of Kaposi's sarcoma-associated herpesvirus (human herpesvirus 8) in culture. Nat. Med. **2:**342–346.

57. **Samols, M. A., J. Hu, R. J. Skalsky, and R. Renne.** 2005. Cloning and identification of a microRNA cluster within the latency-associated region of Kaposi's sarcoma-associated herpesvirus. J. Virol. **79:**9301–9305.

58. **Sarid, R., O. Flore, R. A. Bohenzky, Y. Chang, and P. S. Moore.** 1998. Transcription mapping of the Kaposi's sarcoma-associated herpesvirus (human herpesvirus 8) genome in a body cavity-based lymphoma cell line (BC-1). J. Virol. **72:**1005–1012.

59. **Soulier, J., L. Grollet, E. Oksenhendler, P. Cacoub, D. Cazals-Hatem, P. Babinet, M. F. d'Agay, J. P. Clauvel, M. Raphael, L. Degos, et al.** 1995. Kaposi's sarcoma-associated herpesvirus-like DNA sequences in multicentric Castleman's disease. Blood **86:**1276–1280.

60. **Staskus, K. A., W. Zhong, K. Gebhard, B. Herndier, H. Wang, R. Renne, J. Beneke, J. Pudney, D. J. Anderson, D. Ganem, and A. T. Haase.** 1997. Kaposi's sarcoma-associated herpesvirus gene expression in endothelial (spindle) tumor cells. J. Virol. **71:**715–719.

61. **Staudt, M. R., Y. Kanan, J. H. Jeong, J. F. Papin, R. Hines-Boykin, and D. P. Dittmer.** 2004. The tumor microenvironment controls primary effusion lymphoma growth in vivo. Cancer Res. **64:**4790–4799.

62. **Stewart, S. A., and R. A. Weinberg.** 2000. Telomerase and human tumorigenesis. Semin. Cancer Biol. **10:**399–406.

63. **Talbot, S. J., R. A. Weiss, P. Kellam, and C. Boshoff.** 1999. Transcriptional analysis of human herpesvirus-8 open reading frames 71, 72, 73, K14, and 74 in a primary effusion lymphoma cell line. Virology **257:**84–94.

64. **Wang, H. W., M. W. Trotter, D. Lagos, D. Bourboulia, S. Henderson, T. Makinen, S. Elliman, A. M. Flanagan, K. Alitalo, and C. Boshoff.** 2004. Kaposi sarcoma herpesvirus-induced cellular reprogramming contributes to the lymphatic endothelial gene expression in Kaposi sarcoma. Nat. Genet. **36:**687–693.